EVALUATION OF RATE CONSTANTS RELAVANT TO THE HYPERGOLIC REACTION OF HYDRAZINE WITH NITROGEN DIOXIDE

Y. Daimon*, H. Terashima and M. Koshi****
koshi@rocketlab.t.u-tokyo.ac.jp
*Japan Aerospace Exploration Agency, 2-1-1 Tsukuba, Ibaraki, 305-8050, Japan
**The University of Tokyo, 7-3-1 Hongo, Bunkyo-ku, Tokyo, 113-8656, Japan

Abstract
Hydrazine (N_2H_4) has a unique characteristic of inducing hypergolic ignition even at very low temperatures with many oxidizers, such as nitrogen dioxide (NO_2). The elementary reactions of N_2H_4+NO_2 and its consecutive reactions are expected to be a key for the understanding of hypergolic nature. In this study, extensive quantum chemical calculations were performed at the CBS-QB3 level of theory for possible sequential reactions of N_2H_4+NO_2=N_2H_3+HONO (1), N_2H_3+NO_2=$N_2H_3NO_2$=N_2H_2+HONO (2), N_2H_2+NO_2=NNH +HONO (3), and NNH+NO_2= N_2+HONO (4). Activation barriers for those reactions were found to be low or zero, and overall exo-thermicity of the sequential reactions is very large because of the final production of N_2. The reaction (2) proceeds through a stable complex, $N_2H_3NO_2$, and its rate constant depends on pressure (a chemical activation reaction). Rate constants of the reactions (1)-(4) were evaluated by using a transition state theory and a master equation analysis for pressure dependent reactions. A detailed chemical kinetic mechanism for the N_2H_4/NO_2 gas phase combustion was preliminary constructed considering those four sequential reactions. Results show that this proposed mechanism explains possible ignitions of N_2H_4/NO_2 at low temperatures and the proposed sequential reactions (1)-(4) play an important role for the hypergolic nature of N_2H_4/NO_2 combustion at low temperature.

Introduction
A bipropellant combination frequently used in aerospace vehicles is hydrazine (N_2H_4) as a fuel and nitrogen tetroxide (N_2O_4), in fact the NO_2-N_2O_4 equilibrium, as an oxidizer. This combination is known to be hypergolic around room temperature and has been extensively studied experimentally [1-7].

Because of the hypergolic nature, it is quite difficult to obtain detailed information on the elementary chemical kinetics of N_2H_4 combustion. Lawyer [1] investigated the combustion of N_2H_4 droplets burning in N_2O_4 vapor using a suspended droplet technique. It was found that the temperature of the N_2H_4 droplets remained at the boiling point during steady state burning, and the N_2H_4 droplets burned with two flames: an inner decomposition flame and an outer oxidation flame. The results indicate that the combustion of N_2H_4 takes place in the gas phase with a main oxidizer of NO_2. Sawyer and Glassman [3] studied gas phase reactions of N_2H_4 with O_2, NO, and NO_2. They found that two-stage combustion consists of fast and slow temperature rises, where combustion with NO_2 was fastest and its reaction rate was much faster than N_2H_4 decomposition. They stated that the high reactivity of N_2H_4 and NO_2 was not the result of a chain-branching mechanism, but was attributed to the high effectiveness of NO_2 in hydrogen abstraction. However, there is no chemical kinetic information on the rate of hydrogen abstraction reaction of NO_2 from N_2H_4. Daimon el al. [5-7] observed N_2H_4 droplet combustion, which was dropped into liquid N_2O_4. They found that a

dispersed layer at the depressed N_2O_4 surface was formed just before the beginning of the explosion. They stated that sudden gasification of a superheated liquid layer formed at the boundary of two liquids occurred spontaneously and a detonation-like violent reaction proceeded.

Those previous studies indicate that the hypergolic initiation of N_2H_4/N_2O_4 system occurs in the gas phase. After the vaporization of N_2O_4 liquid, the equilibrium between N_2O_4 and NO_2 largely exceeds to NO_2. Therefore, the hypergolic ignition could be explained by the gas phase chemical reactions between N_2H_4 and NO_2.

Compared to experimental investigations, analytical studies on chemical kinetics of N_2H_4 combustion are very limited. Catoire et al. [8] developed a detailed chemical kinetic mechanism of N_2H_4 decomposition for the simulation of detonation in pure N_2H_4. This mechanism consists of 13 chemical species and 33 elementary reactions. Konnov and Ruyck [9] proposed a kinetic mechanism for the decomposition of N_2H_4. Their mechanism consists of 11 species and 51 reactions and widely validated against shock tube ignition delay data and flame speed data. To our best of knowledge, however, only one chemical kinetic mechanism has been published for the N_2H_4/NO_2 combustion. Ohminami et al. [10,11] extensively compiled literature data of chemical kinetics relevant to N_2H_4/N_2O_4 combustion. Their mechanism contained 30 chemical species and 245 elementary reactions, in which combustion proceeds on the chain branching mechanism initiated by the production of radicals from thermal decomposition of reactants. Since decomposition of reactants could not occur at low temperatures, the mechanism fails to explain the low temperature auto-ignition.

According to the experiments on the gas phase combustion by Sawyer and Glassman [3], non-chain and direct reactions between N_2H_4 and NO_2, which may be the hydrogen abstraction by NO_2, might play an important role on the auto-ignition of N_2H_4/NO_2 system. However, there has been no available kinetic data on this reaction.

In this study, possible reaction pathways between N_2H_4 and NO_2 are extensively explored by using *ab-initio* quantum chemical calculations. Rate constants of the reactions are evaluated on the basis of the transition state theory (TST). Reaction pathways and their rate constants for the consecutive processes are also examined. The reactions of N_2H_3 produced by the hydrogen abstraction are found to proceed via the formation of a stable intermediate (adduct) and rates of these reactions might be pressure dependent. The master equation analysis is also performed to evaluate the rate constant of these pressure dependent reactions. Elementary reactions studied are implemented into a chemical kinetic mechanism of N_2H_4 combustion and simulations are performed for examining the hypergolic reaction at low temperature. In the next section, the chemical kinetic mechanism for N_2H_4/NO_2 reaction and source of the thermochemical data are briefly described before the discussion of each elementary reaction.

Reaction mechanism

A chemical kinetic mechanism for the N_2H_4/NO_2 combustion has been developed by modifying the mechanism originally proposed by Ohminami et al. [10,11]. The modified mechanism (hereafter, mechanism A) consists of 33 species and 239 reactions. Most of elementary reactions for N-H species and their rate constants in the mechanism were taken from Dean and Bozzelli [12]. The subset of H_2 combustion in the mechanism of Ohminami is replaced by a recent mechanism proposed by an author [13], which is appropriate for high-pressure conditions. It is noted that some of the rate constants for the pressure dependent reactions in ref. 12 are only given at p=0.1, 1 ant 10 atm. Those reactions include dissociation of N_2H_4, N_2H_3, and N_2H_2, isomerization of N_2H_2 (HNNH) to H_2NN, and chemical activation reactions of $NH_2+NH_2 = N_2H_3+H$, $NH_2+NH_2=H_2NN+H_2$. In the present study, a target pressure is fixed to p=10 atm, and values of these rate constants in ref.12 are used.

Thermochemistry

The thermochemical properties of the species involved in the mechanism A were mostly extracted from the comprehensive thermochemical database proposed by Burcat and Rusic [14]. Other sources of thermochemical data are the CHEMKIN-II library [15] and the review of Dean and Bozzelli [12]. In the present study, since some of the species, such as the gaseous species $N_2H_3NO_2$ (which is likely to be formed form the reaction of N_2H_3 and NO_2), are not available in those databases, thermochemical properties (heat capacity, entropy, and enthalpy) are obtained on the basis of ab-initio quantum chemical calculations. Geometry of those species is optimized at the B3LYP/6-311++G (3df, 3pd) level of theory, and its energies are calculated by CBS-QB3 method. Heat of formation is calculated by using ARM1 method proposed by Asatryan et al. [16]. Results are compared in Table 1 with other database values. Thermochemical properties are calculated by using a program suite GPOP (Gaussian post processor) developed by Miyoshi [17].

Table 1. Heat of formation (kcal/mol)

Species	Ref.12	Ref.14	Ref.15	CBS-QB3
N_2H_2	49.83	50.47	50.9	47.96
H_2NN	–	–	–	71.22
N_2H_3	47.95	52.57	36.77	53.86
N_2H_4	22.73	22.67	22.78	23.75
HNO	25.32	25.44	23.79	24.499
HON	60.79	–	–	66.72
HNNO	–		–	46.76
HNOH	21.53	–	21.05	21.99
HONO	−18.5	–	−18.31	−20.1
HNOO	56.1	–	–	56.72
HNO_2	−14.1	−18.69	14.15	−12.29
NH_2O	15.84	15.78	–	14.22
NH_2NO	17.84	–	–	17.84
NH_2OH				−11.12
N_2H_3ONO				41.19
$N_2H_3NO_2$				22.89

Evaluation of rate constants

Search of reaction pathways for the N_2H_4+NO_2 and its consecutive reactions have been performed at the B3LYP/6-311++G(3df, 3pd) level of theory. Transition states are extensively searched and if a transition state (TS) was found, IRC (intrinsic reaction coordinate) calculation was conducted in order to assign reactants and products of this TS. Energies of those stationary states were calculated by CBS-QB3 method. All calculations were performed by using GAUSSIAN 03 program suite. Rate constant for the reaction having TS was calculated by using GPOP [17]. GPOP program suite can also be used for the reaction without TS such as N_2H_3+NO_2 on the basis of VTST (variational TST). A master equation analysis for dissociation and chemical activation reactions was performed by using a SSUMES (Steady-State Unimolecular Master-Equation Solver) developed by Miyoshi [18].

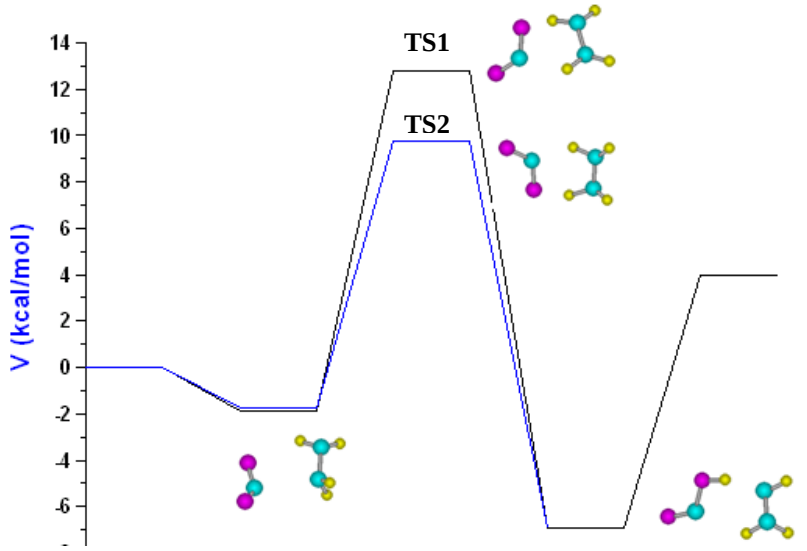

Figure 1. Energy diagram of N_2H_4+NO_2 reactions. (CBS-QB3)

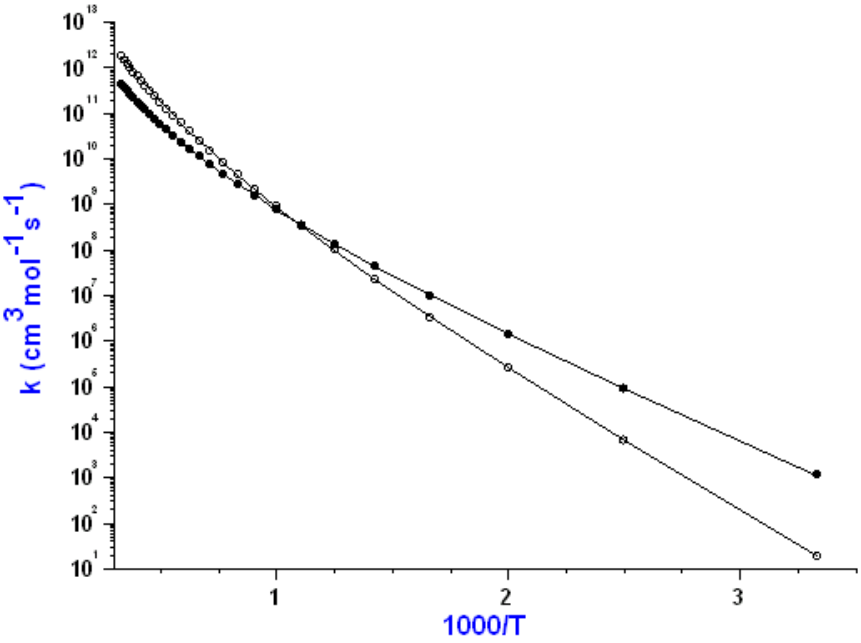

Figure 2. Rate constants for the N_2H_4+NO_2 reaction. A curve with open circles: TS1, with closed circles:TS2.

(1) N_2H_4+NO_2=N_2H_3+HONO

This can be the initiation of N_2H_4/NO_2 hypergolic explosion. The reaction is endothermic by 3.98 kcal/mol (based on CBS-QB3 energy at 0K). Since NO_2 is a radical, relatively low activation barrier is expected. Indeed, two TSs are found with activation barrier of 12.82 (TS1) and 9.77 (TS2) kcal/mol, respectively. Energy diagram is shown in Fig.1. IRC calculations indicate those TSs correlate to stable adducts on both reactant and product side, as shown in Fig.1. Both TS1 and TS2 correlate the same adduct on product side with the energy of -6.92 kcal/mol. Adducts on reactant side are different from each other for TS1 and TS2, though the energy is very similar (-1.87 and -1.74 kcal/mol for TS1 and TS2 channels, respectively). A simple TST calculation was performed in the present study by neglecting the existence of these adducts. Resulting rate constants are depicted in Fig. 2. The rate constants are corrected for tunneling by assuming asymmetric Eckart potential [19], but these

corrections are negligible because of rather loose TS (imaginary frequencies of 708 and 332 cm^{-1}, for TS1 and TS2, respectively). Following modified Arrhenius expressions are obtained.

$$TS1: \quad k = 48.9 \times T^{3.43} \exp(-5566/T)$$
$$TS2: \quad k = 12.0 \times T^{3.23} \exp(-4076/T) \quad cm^3 mol^{-1} s^{-1}$$

Another TS with the barrier height of 9.27 kcal/mol was also found, but this TS correlates to different products, N_2H_3+HNO_2 which is 12.0 kcal/mol endothermic. No further study was performed for this pathway because of its higher endothermicity.

(2) N_2H_3+NO_2=$N_2H_3NO_2$=N_2H_2+HONO

N_2H_3 produced by the reaction (1) will further react with NO_2. Since both N_2H_3 and NO_2 are radicals, recombination products are expected to form without any energy barrier. Two isomers, $N_2H_3NO_2$ (ΔH=-35.79 kcal/mol) and N_2H_3ONO (ΔH=-17.82 kcal/mol), are possible for the recombination of N_2H_3 and NO_2. Production of those adducts without energy barrier was confirmed by performing scanning calculations of the potential energy surface. $N_2H_3NO_2$ further decomposes to yield a reduced product (N_2H_2), whereas N_2H_3ONO will produce an oxidation product (N_2H_3O). A primary concern in the present study is the exothermic process of the initial stage of N_2H_4 reaction, and the fate of $N_2H_3NO_2$ was searched in detail. Investigation of consecutive reactions of N_2H_3ONO is open for future studies.

Two TSs were found for the decomposition of $N_2H_3NO_2$ to produce N_2H_2 and HONO. One (Channel-1) leads to formation of t-N_2H_2+HONO with a barrier height of 28.46 kcal/mol (measured from $N_2H_3NO_2$) and another (Channel-2) is a pathway to produce c-N_2H_2+HONO with a barrier height of 33.14 kcal/mol. Energies of these TSs are below the reactant energy. Energy diagram of these reactions are depicted in Fig. 3. Both channel 1 and 2 are exothermic (ΔH=-32.09 for channel 1 and ΔH=-27.05 kcal/mol for channel 2), and a master equation analysis is required to evaluate the rate constants of these chemical activation reactions.

At first, the high-pressure limiting rate constant for the recombination of N_2H_3+NO_2 was calculated on the basis of VTST method by using the GPOP program suite. The reaction

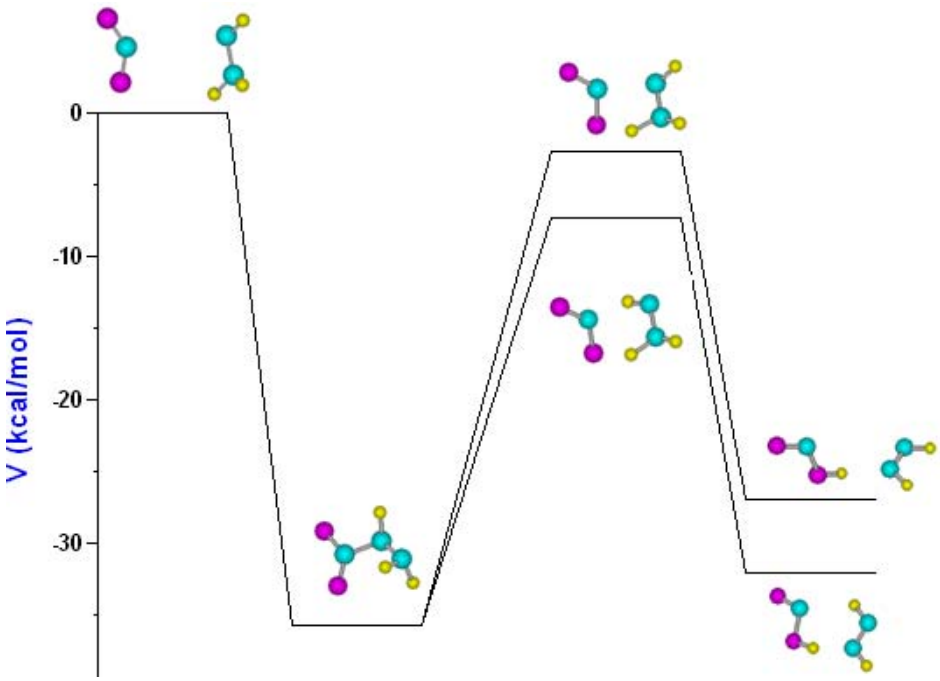

Figure 3. Energy diagram of N_2H_3+NO_2=$N_2H_3NO_2$=N_2H_2+HONO reactions (CBS-QB3).

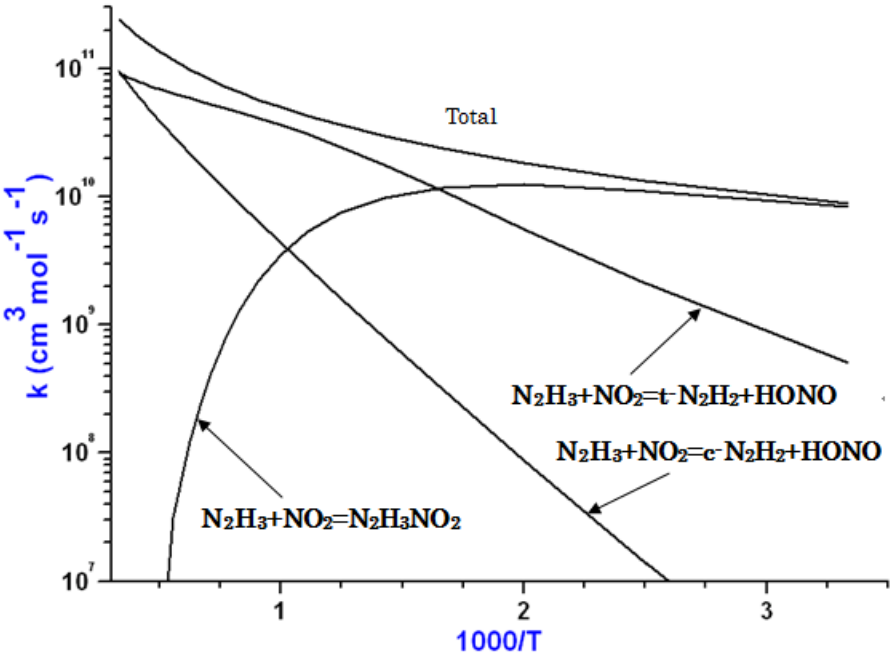

Figure 4. Rate constants for the chemical activation reaction of N_2H_3+NO_2. The 'Total' rate constant is the high-pressure limiting rate constant calculated by VTST. Other three rate constants are obtained by solving master equations at p=10 atm.

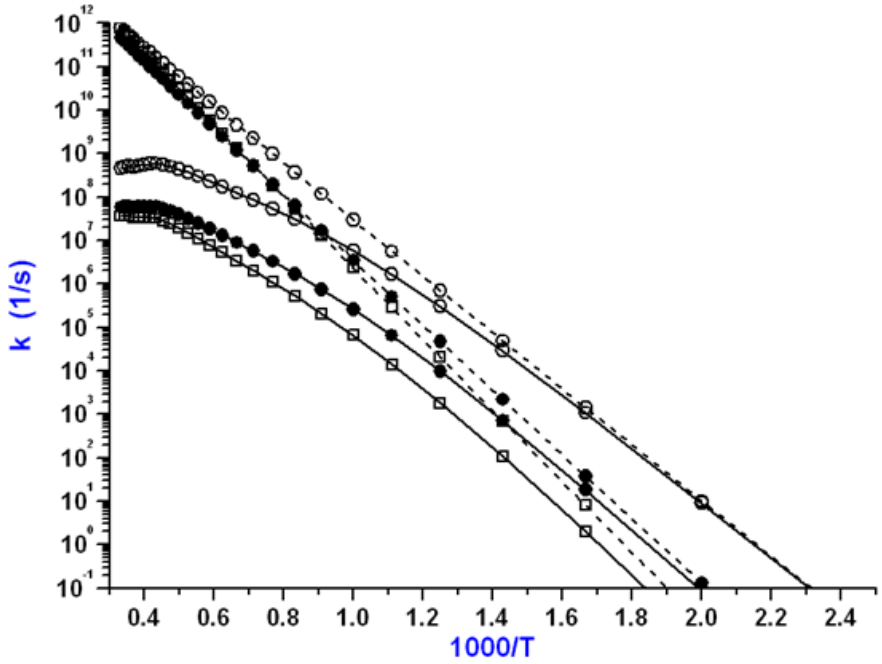

Figure 5. Rate constants of unimolecular dissociation of N2H3NO2. Broken lines are for high-pressure limiting rate constants, solid curves are calculated at p=10 atm. Open circles: $N_2H_3NO_2$=t-N_2H_2+HONO, open squres: $N_2H_3NO_2$=c-N_2H_2+HONO, closed circles: $N_2H_3NO_2$=N_2H_3+NO_2.

coordinate of the recombination was approximated by a N-N bond length in the O_2N-$NHNH_2$ ($N_2H_3NO_2$) molecule, and partial optimization of the structure at the fixed N-N bond length was performed at the B3LYP/6-311++G (3df, 3pd) level of theory. Vibrational frequencies and principle moments of inertia on each position of reaction coordinate were used to calculate the micro-canonical rate constant, k(E), for the recombination reaction of N_2H_3+NO_2. Resulting VTST rate constant (which is the high-pressure limiting rate constant)

is shown in Fig.4 as the 'Total rate constant'. Rate constants of the chemical activation reactions for each of three channels, (channels 1, 2 and recombination channel of $N_2H_3+NO_2$ $=N_2H_3NO_2$) were calculated at p=10 atm by using SSUMES program suite. Results are also depicted in Fig.4.

Rate constants for the unimolecular dissociation of $N_2H_3NO_2$ were also calculated at p=10 atm for the three channels using SSUMES and results are depicted in Fig. 5. Large deviations from high-pressure limiting rate constants at high temperatures are evident in this figure and these are caused by non-equilibrium distributions of internal energy even at p=10 atm. It is noted that such non-equilibrium effect i.e., deviation from high-pressure rate constant, is more notable for the pathway with higher energy barrier.

For kinetic simulations, rate constants at p=10 atm are fitted to modified Arrhenius form as follows.

$N_2H_3+NO_2$=t-N_2H_2+HONO	$k=3.97\times10^{12}T^{-0.39}\exp(-2030/T)$	$cm^3mol^{-1}s^{-1}$
$N_2H_3+NO_2$=c-N_2H_2+HONO	$k=4.57\times10^{8}T^{+0.80}\exp(-3305/T)$	$cm^3mol^{-1}s^{-1}$
$N_2H_3NO_2$ =t-N_2H_2+HONO	$k=1.83\times10^{33}T^{-6.32}\exp(-17406/T)$	s^{-1}
$N_2H_3NO_2$ =c-N_2H_2+HONO	$k=1.05\times10^{34}T^{-6.74}\exp(-20771/T)$	s^{-1}
$N_2H_3NO_2$ =$N_2H_3+NO_2$	$k=1.84\times10^{33}T^{-6.52}\exp(-19154/T)$	s^{-1}

(3) $N_2H_2+NO_2$=NNH+HONO

Both t-N_2H_2 (trans) and c-N_2H_2 (cis) can be produced by the reaction (2), as shown in fig.2, but the production rate of t-N_2H_2 is much faster because of the lower energy barrier height. In the present study, t-$N_2H_2+NO_2$ reaction was implemented in the modified chemical kinetic mechanism. Energy diagram of this reaction is shown in Fig.6. Adducts with shallow potential minima were found both reactant and product paths. The TS has Cs symmetry with its barrier height of 11.88 kcal/mol. The imaginary frequency of this TS is 1509 cm^{-1} and the tunneling effect might be important at lower temperatures. The rate constant obtained with Eckart tunneling correction is as follow.

$k=1.12\times10^{-3}T^{4.47}\exp(-3615/T)$ $cm^3mol^{-1}s^{-1}$

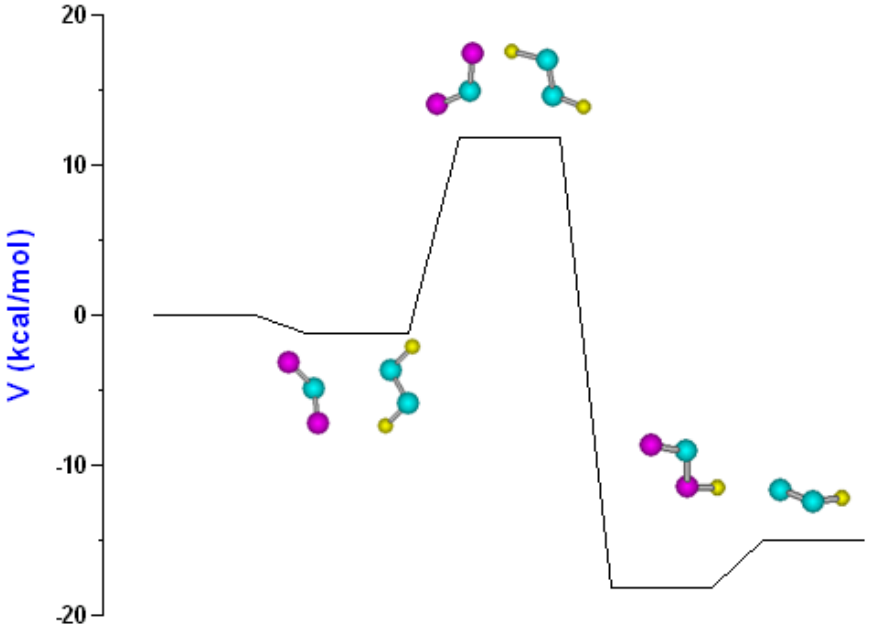

Figure 6. Energy diagram of t-$N_2H_2+NO_2$=NNH+HONO reaction. (CBS-QB3)

(4) $NNH+NO_2=N_2+HONO$

This reaction has very large exothermicity (ΔH=-84.76 kcal/mol) because of the production of N_2. A TS with very low activation barrier (1.93 kcal/mol) was found. The IRC calculation indicated that products of this reaction were N_2 and cis form of HONO, c-HONO, as shown in Fig.7. TST calculation results in the following rate constant.

$$k=17.35xT^{2.84}\exp(-842/T) \quad cm^3mol^{-1}s^{-1}$$

t-HONO is slightly stable than c-HONO, but the difference (0.43 kcal/mol) is small. The barrier height of the isomerization reaction from t-HONO to c-HONO was found to be 10.36 kcal/mol. It is expected that c-HONO produced by the reaction (4) has large excess internal energy because of large exothermicity of the reaction. Therefore, c-HONO produced is readily converted to t-HONO.

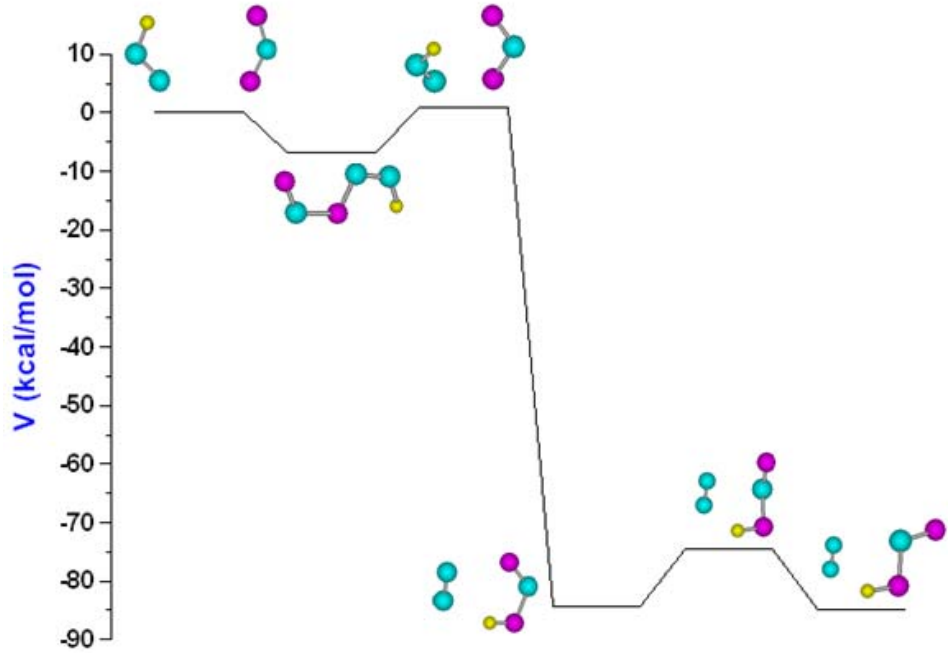

Figure 7. Energy diagram of $NNH+NO_2=N_2+HONO$ reaction. (CBS-QB3)

Kinetic simulation of ignition at p=10 atm

Reactions of $N_2H_4+NO_2$ and subsequent reactions described in the previous sections are implemented into the mechanism A. This modified mechanism (mechanism B) includes the following elementary reactions.

$N_2H_4+NO_2$	$=N_2H_3+HONO$	(1)
$N_2H_3+NO_2$	$=N_2H_3NO_2$	(2a)
$N_2H_3NO_2$	$=N_2H_2+HONO$	(2b)
$N_2H_3+NO_2$	$=N_2H_2+HONO$	(2c)
$N_2H_2+NO_2$	$=NNH+HONO$	(3)
$NNH+NO_2$	$=N_2+HONO$	(4)

Isomers of N_2H_2 and HONO (trans and cis) are not distinguished in the mechanism B and rate constants of reactions (2a), (2b), and (2c) are only given at p=10 atm. Ignition delay times of a N_2H_4/NO_2=3/1 mixture at p=10 atm were calculated for the adiabatic combustion

(with constant enthalpy and pressure). Results are depicted in Fig. 8. The ignition delay times were defined as the time required for the 100 K temperature increase. As can be seen in the figure, the ignition delay times calculated by the mechanism A is much longer than those obtained by the mechanism B. The ignition delay times obtained with the mechanism A below 800 K are longer than 10 second, and practically no ignition is possible. On the other hand, the mechanism B gives the ignition delay time of 2.8 ms at 400 K. This indicates that the reactions of (1)-(4) play an essential role for the hypergolic ignition of N_2H_4 at low temperatures.

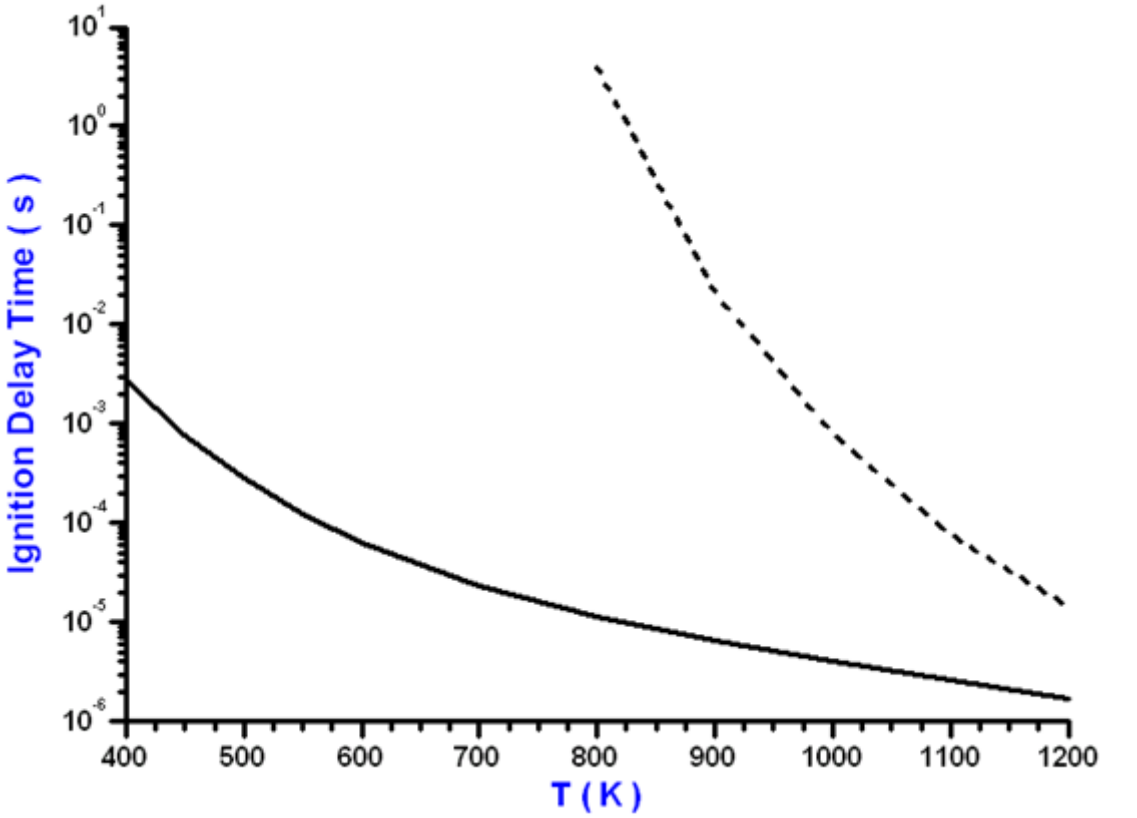

Figure 8. Ignition delay times of N_2H_4/NO_2=3/1 mixture at p=10 atm. Broken line: mechanism A, Solid line: mechanism B.

Concluding remarks

For the understanding of the chemical kinetic origin of the hypergolic ignition of N_2H_4/NO_2 mixture, a preliminary mechanism was constructed. The proposed mechanism can predict possible ignition of N_2H_4/NO_2 even at room temperature. The origin of the low temperature ignition is the reaction sequence of hydrogen abstraction by NO_2 from N_2H_4, N_2H_4=>N_2H_3=>N_2H_2=>NNH=>N_2. Large amount of heat is released during this reaction sequence, and the resulting temperature rise accelerates the reaction (1), which has a small activation barrier.

Although the proposed mechanism successfully predicts the hypergolic ignition of N_2H_4/NO_2 reaction system, the present mechanism is still 'preliminary'. Following problems remain to be solved.

1) Calculations of the rate constants for chemical activation and unimolecular reaction are required at wide range of pressures to obtain the complete mapping of k(T,P).

2) Production of NH_3ONO and its consecutive reactions have to be considered. Those reactions could be important for the oxidation pathways of N_2H_4.

3) Reactions of isomers of N_2H_2 and HONO have to be included, though the importance of those reactions is not clear.

. A study to clarify those problems are now in progress.

References

[1] Lawver, B.R., "Some Observations on the combustion of N2H4 droplets", AIAA J. 4: 659-662 (1966).

[2] Ray, A.B., Koehler, G., Salser, G.E., Dauerman, L., "Evidence for the formation of Azides in the N2H4/N2O4 reaction", AIAA J., 6:21862187 (1967).

[3] Sawyer, R.F., Glassman, I., "Gas-phase reactions of hydrazine with nitrogen dioxide, nitric oxide, and oxygen", Proc. Combust. Inst., 11: 861-869 (1967).

[4] Saad, M.A., Detweiler, M.B., Sweeney, M., "Analysis of reaction products of nitrogen tetroxide with hydrazines under nonignition conditions", AIAA J., 8: 1073-1078 (1972).

[5] Daimon, W., Tanaka, M., Kimura, I., "The mechanisms of explosions induced by contact of hypergolic liquid propellants, hydrazine and nitrogen tetroxide", Proc. Combust. Inst., 20: 2065-2071 (1984).

[6] Tanaka, M., Daimon, W., Kimura, I., "Explosion phenomenon from contact of hypergolic liquids", J. Propulsion Power, 1:314-316 (1984).

[7] Daimon, W., Gotoh, Y., Kimura, I., Mechanism of explosion induced by contact of hypergolic liquids", J. Propulsion, 7:946-952 (1991).

[8] Catoire, L., Luche, J., Dupre, G., Paillard, C., "Critical reactions for the hydrazine vapor detonations", Shock Waves 11:97-103 (2001).

[9] Konnov A.A., Ruyck, J.D., "Kinetic modeling of the decomposition and flames of hydrazine", Comb. Flame 124:1060126 (2001).

[10] Ohminami, K., Ogawa, H., Hayashi, A.K., "Development of a reduced chemical kinetic model of hydrazine and di-nitrogen tetroxide", Sci. Tech. Energetic Materials 69:1-7 (2008) (in Japanese)..

[11] Ohminami, K., Sawai, S., Uesugi, T. K., Yamanishi, N., Koshi, M., "Hydrazine and di-Nitorogen Tetroxide Combustion Model inside Film-Cooled Bipropellant Thruster", 45th AIAA/ASME/SAE/ASEE Joint Propulsion Conference & Exhibit, AIAA-2009-5044 (2009).

[12] Dean, A.M., Bozzelli, J.W., "Combustion chemistry of nitrogen", in Gas Phase Combustion Chemistry, ed. by Gardiner, W.C.Jr., Springer-Verlag, New-York (2000).

[13] Shimizu, K., Hibi, A., Koshi, M., Morii, Y., Tsuboi, N., "Updated kinetic mechanism for high-pressure hydrogen combustion", J. Propulsion Power 27:383-395 (2011).

[14] Brucat, A., Ruscic, B., "Third millennium ideal gas and condensed phase thermochemical database for combustion with updates from active thermochemical tables", ANL-05/20, TAE960 (2005).

[15] Kee, R.J., Eupley, F.M., Miller, J.A., "The Chemkin thermodynamic data base", Sandia National Laboraatories Report SAND87-8215B (1987).

[16] Asatryan, R., Bozzelli, J.W., Simmie, J.M., "Thermochemistry of methyl and ethyl nitro, RNO_2, and nitrite, RONO, organic compounds", J. Phys. Chem., 112:3172-3185 (2008).

[17] Miyoshi, A., http://www.frad.t.u-tokyo.ac.jp/~miyoshi/gpop/

[18] Miyoshi, A., http://www.frad.t.u-tokyo.ac.jp/~miyoshi/ssumes/

[19] Garrett, B.C., and Truhlar, D.G., "Semiclassical tunneling calculations", J. Phys. Chem., 83:2921-2926 (1979).